Journal of Organometallic Chemistry, 450 (1993) 165–170

JOM 23289

Electrochemical and chemical generation of a mixed-valent organorhenium oxide and its subsequent aggregation

Rolf W. Albach, Ulrich Küsthardt, Joachim Behm and Birgit Ebert

Lehrstuhl für Anorganische Chemie I, TU München, Lichtenbergstr. 4, W-8046 Garching (Germany)

Marie-Helène Delville and Didier Astruc

Laboratoire de Chimie Organique et Organometallique, Université de Bordeaux I, 351 cours de la Libération, F-33405 Talence Cedex (France)

(Received August 7, 1992)

Abstract

Electrochemical one-electron reduction of the dinuclear d^1–d^1 organorhenium oxides $Me_4Re_2O_4$ (**1**) and (c-Pr)$_4$Re$_2$O$_4$ (**2**) reversibly yields the mono-anions $\mathbf{1}^-$ and $\mathbf{2}^-$. Further electrochemical reduction is irreversible. The observed mechanisms upon electrochemical reduction and the involved electrode kinetics are discussed in the light of the electrochemical data. Chemical reduction by cobaltocene leads quantitatively to the same dinuclear radical complexes $\mathbf{1}^-$ and $\mathbf{2}^-$, the EPR spectra of which support the formulation as $Re^{V}Re^{VI}$ mixed-valence dimers. Reoxidation can be achieved with ferricinium hexafluorophosphate. Upon controlled exposure to oxygen the extraordinarily air-sensitive anion $\mathbf{1}^-$ forms the unprecedented linear trinuclear rhenium cluster $[Cp_2Co][Me_6Re_3O_6]$ (**4**). The mechanism of this aggregation reaction involving disproportionation is discussed. The crystal and molecular structure of the anion **4** has been determined, the trimeric anion has almost C_{2v} symmetry, and the Re–Re–Re angle is nearly linear (177.83(2)°).

1. Introduction

Transition metal oxides are of great importance as catalysts in nature and in industrial chemistry [1]. Oxorhenium compounds, in particular, are of potential use in homogeneous and heterogeneous catalysis [2]. Organometallic rhenium oxides are excellent models for compounds involved in the catalytic cycles. Therefore, extensive studies of their chemical, spectroscopic and redox properties are necessary for understanding the reactivity patterns observed for this fascinating class of organometallic compounds. Little has been done towards understanding of the electrochemistry of organorhenium complexes in high oxidation states [3]. Electrochemical reductions of all rhenium(VII) oxides lead irreversibly to lower valent rhenium compounds [4]. On a preparative scale no single product has yet been isolated. Similar observations can be made with respect to organometallic rhenium(V) oxides [5].

The chemistry of oxo-rhenium-alkyls is governed by the complex influence of the electronical requirements on the one hand and steric features on the other. Support for this statement is provided by the electrochemical comparison of three similar dinuclear d^1–d^1 organorhenium oxides: $Me_4Re_2O_4$ (**1**) [6], (c-Pr)$_4$Re$_2$O$_4$ (**2**) [7] and $Np_4Re_2O_4$ (**3**) [8] (Me = methyl; c-Pr = cyclo-propyl; Np = neopentyl), which upon electrochemical and chemical reduction give clearly different types of product. Furthermore, the stabilities of the reduction products towards dioxygen differ significantly.

2. Experimental details

2.1. Syntheses

All syntheses were performed under argon by standard Schlenk techniques. All solvents were deaerated,

---

Correspondence to: Dr. U. Küsthardt.

0022-328X/93/$6.00

dried and distilled before use. The water content was found to be < 2 ppm.

2.2. Starting materials

Dirhenium heptoxide was used as supplied commercially. Tetramethyltetraoxodirhenium [9], $Me_4Re_2O_4$ (**1**) was prepared by reductive alkylation of dirhenium heptoxide with methyltrisisopropylatotitanium [10]. Thus 1.83 g (3.78 mmol) of Re_2O_7 was dispersed in 50 ml of THF at 0°C and 3.08 g (12.8 mmol) of $CH_3Ti(OCH(CH_3)_2)_3$ in 15 ml THF was added slowly and the solution refluxed for 3 h. The product was purified by filtration through silylated silica gel and subsequent vacuum sublimation (yield 35%). Tetrakiscyclopropyltetraoxodirhenium (**2**) was prepared by reductive alkylation of dirheniumheptoxide with $Zn(c\text{-}Pr)_2$, as described elsewhere [7].

2.3. Cobaltoceniumtetramethyltetraoxodirhenate (V / VI) (1^-)

To a solution of 210 mg (0.42 mmol) of $Me_4Re_2O_4$ (**1**) in pentane, 79.8 mg of cobaltocene (0.42 mmol) in 10 ml of pentane was added with vigorous stirring at 293 K. The green precipitate was filtered off and washed with 10 ml each of pentane and ether. Yield: 230 mg (80%). IR (KBr, cm^{-1}): 975, 954 (ν(Re=O)). EPR (in KBr, 4 K): $\langle g \rangle = 1.811 \pm 0.0025$, linewidth 59.4 mT. Anal. Found: C, 23.80; H, 3.22; Re, 52.11; Co, 8.21. $C_{14}H_{22}CoO_4Re_2$ calc.: C, 24.52; H, 3.23; Re, 54.31; Co, 8.59%. Chronoamperometric measurements ($c_0 = 3 \cdot 10^{-6}$, $A = 7.9 \cdot 10^{-3}$ cm^2): $i^2t = 5.83 \cdot 10^{-11} \pm 0.03 \cdot 10^{-11}$ A^2 s. The diffusion coefficient (D) was calculated to be $3.45 \cdot 10^{-5}$ cm^2 s^{-1}.

2.4. Cobaltoceniumtetrakiscyclopropyltetraoxodirhenat (V / VI) (2^-)

To a solution of 140 mg (0.233 mmol) of $c\text{-}Pr_4Re_2O_4$ (**2**) in pentane, 90 mg of cobaltocene (0.476 mmol) in 10 ml pentane was added with vigorous stirring at 293 K. The green precipitate was filtered off and washed with 10 ml each of pentane and ether. The filtrate and the washings contained 40 mg of cobaltocene (0.21 mmol). IR (KBr, cm^{-1}): 956, 946 (ν(Re=O)); 872, 862 (ν(Re–μ-O)). Anal. Found: Re, 41.96; Co, 6.8 (Re/Co = 1.95). $C_{22}H_{30}CoO_4Re_2$ calc.: Re, 47.15; Co, 7.46%.

2.5. Cobaltoceniumhexamethylhexaoxotrisrhenate(VI / V / VI) (4)

A solution of 75 mg of cobaltocene (0.4 mmol) in 5 ml of THF was added to 200 mg (0.4 mmol) of $Me_4Re_2O_4$ (**1**) in 5 ml of THF at 293 K, and 30 ml (excess) of air was introduced. The solution was stirred for 3 h, the precipitate filtered off, washed with THF, and was identified as cobaltocenium perrhenate. The red filtrate was evaporated, and the residue recrystallized from THF/n-pentane to give 160 mg (86%) of **4** as red crystals. ^1H NMR (THF-d_8, ppm): 6.00 (s, 10H); 1.97 (s, 12H); 1.81 (s, 6H). Conductivity (MeCN, $3 \cdot 10^{-4}$ M, 20°C): 172 S mol^{-1} cm^{-2}. IR (KBr, cm^{-1}): 998, 910 (ν(Re=O)). FT-Raman (cm^{-1}): 995, 961 (ν(Re=O)); 189, 135 (ν(Re–Re)). FD^--MS (m/e): 741.3 (M^-, ^{185}Re). Cyclic voltammetry (MeCN): −1.91 V (quasi-reversible).

2.6. Instrumentation

Electrochemical measurements were performed on a PAR 173/276 potentiostat (EG&G) with a specially developed CV software program [11]. Cyclic voltammetry (CV) was performed by use of a three-electrode configuration [4] consisting of a highly polished glassy carbon disk working electrode ($A = 7$ mm^2) (Metrohm), a Pt auxiliary electrode, and a Ag/AgCl reference electrode. The working compartment of the electrochemical cell was separated from the reference compartment by a Luggin capillary. All three compartments contained a 0.1 M solution of tetrabutylammonium hexafluorophosphate (TBAP) (Aldrich) as a supporting electrolyte. All solutions used for the electrochemical experiments were carefully dried, stored under argon, and before use stirred for more than 1 h over activated alumina. Background CV spectra of the blank electrolyte solution were always recorded. Potentials are reported *vs.* aqueous Ag/AgCl/3 M KCl and were standardized against ferrocene (THF, 298 K: 0.535 V *vs.* Ag/AgCl; CH_3CN, 296 K: 0.528 V *vs.* Ag/AgCl). EPR spectra were obtained with a JEOL JES RE2X spectrometer using the Esprit 330 data system at X band frequencies. The microwave frequency was determined with a R5372 frequency counter (Advantest) and the magnetic field was calibrated with an internal MnO marker.

2.7. X-Ray crystallography

Crystals of compound **4** were grown from a THF/Et_2O solution. The crystal data and experimental details of the structure determination, solution and refinement are given in Table 2. The data were collected on an Enraf–Nonius CAD4 four-circle diffractometer using graphite-monochromated Mo Kα radiation. The structure of compound **4** was solved by Patterson methods and refined by full-matrix-least-squares methods. Scattering factors were taken from ref. 12. Anomalous dispersion was taken into account [13]. All calculations were performed on a Microvax 3100 computer with STRUXIII.

The final atomic coordinates for non-hydrogen atoms are listed in Table 3. A table of thermal parameters, a complete list of bond lengths and angles, and a list of hydrogen atom coordinates are available from the Fachinformationszentrum Karlsruhe, Gesellschaft für wissenschaftlich-technische Information mbH, W-7514 Eggenstein-Leopoldshafen 2 (Germany), by quoting the depository number CSD 54901.

3. Results and discussion

3.1. Electrochemistry

All organometallic rhenium(VI) oxides we investigated [14] are quasi-reversibly reduced by one electron between -0.2 and -0.75 V *vs.* Ag/AgCl. No electrochemical oxidations were observed at potentials less than 1.5 V, except in the case of $Mes_2Re^{VI}O_2$, which is oxidized at 0.9 V *vs.* Ag/AgCl [4]. The reduction potentials for the dimeric compounds **1–3** are listed in Table 1.

The energy of the LUMO in each of those dimers decreases in the order $\mathbf{3} \gg \mathbf{1}$ ($\Delta = 0.2$ V, CH_3CN) and $\mathbf{2} > \mathbf{1}$ ($\Delta = 0.07$ V, THF), which is the inverse of the order of the electronreleasing effects of the ligands. A possible explanation is that the metal–alkyl bonds have no influence on the LUMO.

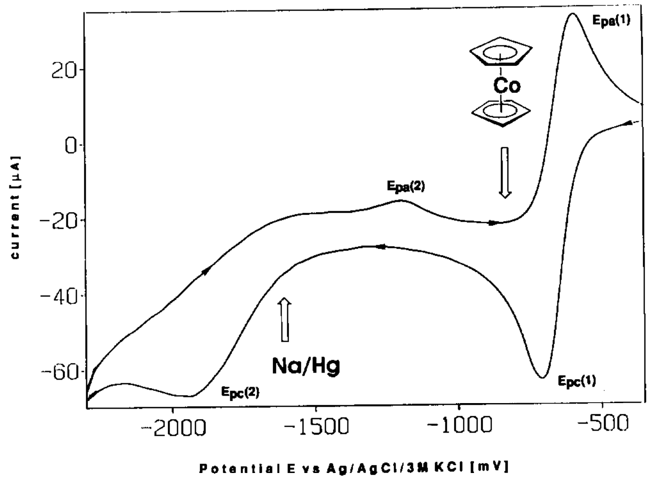

Fig. 1. Cyclic voltammogram of $Me_4Re_2O_4$ (1) in MeCN/0.1 M Bu_4NPF_6 at 297 K; scan rate: 100 mV s^{-1}.

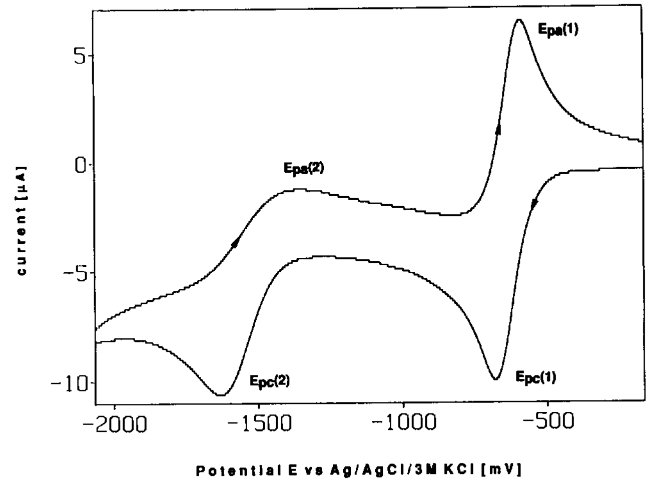

Fig. 2. Cyclic voltammogram of c-$Pr_4Re_2O_4$ (2) in MeCN/0.1 M Bu_4NPF_6 at 297 K; scan rate: 20 mV s^{-1}.

The peak current ratios reveal the electrochemical stability of the radical anion formed upon reduction; $i_{pa}/i_{pc} = 0.95 \pm 0.05$ (0.04 and 0.8 V s^{-1}). At slower scan rates (0.02 V s^{-1}) the ratio decreases to $i_{pa}/i_{pc} = 0.83 \pm 0.05$. Assuming monomolecular consecutive reactions, the transformation rate of $\mathbf{1}^-$ is calculated as $k \leq 0.012 \pm 0.004$ s^{-1}; $t_{1/2} \geq 1$ min [15].

According to the peak-potential differences all the reductions are quasi-reversible. Analysis of the peak potential differences and chronoamperometric current–time curves yields the kinetic parameter Ψ and the diffusion coefficient D [16*]. Assuming a one-electron transfer, the heterogeneous electron transfer rate (k_s^0) is then calculated to be $3.2 \cdot 10^{-2}$ cm s^{-1} [17*]. A two-electron process would involve far slower electrode kinetics and is therefore strongly disfavoured. Furthermore, the appearance of a second wave strongly supports the interpretation as a classical EEC-process [18]. The peak potentials $E_{pc}(2)$ and $E_{pa}(2)$ are summarized in Table 1.

TABLE 1. Electrochemical data for dimeric Re^{VI}-alkyl complexes *vs.* Ag/AgCl/3 M KCl

Compound	$E_{1/2}$ [a] (V)	$E_{1/2}$ [b] (V)	ΔE [d] (mV)	$E_{pc}(2)$ [e]		$E_{pa}(2)$ [f] (V)
				C_E (V)	m_E (V)	
$Me_4Re_2O_4$	-0.71	-0.61	139	-2.58	0.11	-1.18
(c-Pr)$_4Re_2O_4$	-0.64	–	120	-2.38	0.14	-1.25
$Np_4Re_2O_4$ [c]	-0.42	–	–	–	–	–

[a] $E_{1/2} = (E_{pc}(1) + E_{pa}(1)) \cdot 0.5$; condition: 0.1 M Bu_4NPF_6 in THF at 297 K. [b] $E_1/_2 = (E_{pc}(1) + E_{pa}(1)) \cdot 0.5$; condition: 0.1 M Bu_4NPF_6 in CH_3CN at 297 K. [c] -0.64 V *vs.* SCE; 0.1 M Bu_4NClO_4 in CH_3CN; see ref. 8; ferrocene as reference was used to relate potentials *vs.* SCE to those *vs.* Ag/AgCl/3 M KCl: A.J. Bard and L.R. Faulkner, *Electrochemical methods*; Wiley, New York, 1980, p. 701. [d] At scan rate: 100 mV s^{-1} in CH_3CN. [e] $E_p = C_E + m_E \cdot \log v$. [f] At scan rate: 50 mV s^{-1}.

---

* Reference number with asterisk indicates a note in the list of references.

3.2. Formation of Re^VRe^{VI} mixed-valence dimers

For synthesis the reduction potentials $E_{pc}(2)$ for both of the compounds **1** and **2** are accessible by use of amalgams of alkali metals. Reduction of **3** by lithium amalgam yields the four-coordinate $[Np_2ReO_2]^-$ anion, corresponding to transfer of two electrons to the Re–Re dimer [8]. Analogous two-electron reductions of **1** and **2** did not yield any stable product.

As indicated by cyclic voltammetry, a selective reducing agent with an oxidation potential between −0.7 and −1.3 V, such as cobaltocene (−0.82 V, MeCN), is required for a one-electron transfer reaction. Addition of one equivalent of a cobaltocene solution in hydrocarbons to a solution of **1** or **2** immediately gives a green precipitate in quantitative yield. The green compounds are EPR-active and display complicated EPR spectra, as expected for the metal-centred Re^{VI}–Re^V mixed-valence radial anions, $[Cp_2Co][Me_4Re_2O_4]$ (**1**$^-$) and $[Cp_2Co][c\text{-}Pr_4Re_2O_4]$ (**2**$^-$) respectively (Fig. 3). Simulation of the spectra firmly excludes the formation of monomeric species. The Re–O vibrations have shifted to lower wavenumbers (974 and 954 cm^{-1} for **1**$^-$; 1017 and 1007 cm^{-1} for **1**), indicating a significant decrease in the bond order. The ν(Re=O) vibrations $[Np_2ReO_2]^-$ are found at even lower wavenumbers (939, 870 cm^{-1}), thus disfavouring a similar structure for **1**$^-$ or **2**$^-$.

The reversibility of the reduction of **1** in cyclic voltammetry is reproduced by using one equivalent of ferricinium hexafluorophosphate as a typical "outer-sphere" oxidant. Upon reaction of $[Cp_2Co][Me_4Re_2O_4]$ with the ferricinium salt, starting material **1**, ferrocene, and cobaltocenium hexafluorophosphate are obtained.

3.3. Aggregation reaction

At ambient temperature $[Cp_2Co][Me_4Re_2O_4]$ is extremely sensitive to dioxygen: a green solution containing the mixed-valent dimer immediately turns red. Addition of 0.78 equivalent of air to a THF solution of **1**$^-$ at 195 K results in the formation of cobaltocenium perrhenate and a red compound (**4**) that exhibits electrical conductivity in acetonitrile solution ($\Lambda = 175.0$ S cm^{-2} mol^{-1}) [19*] typical of a 1:1 electrolyte [20]. This compound has been characterized by electronic, IR, Raman, and ^{1}H NMR spectroscopy, as well as by FD-mass spectrometry. Electrochemical reduction of **4** leads in a quasi-reversible one-electron step (−1.91 V *vs.* Ag/AgCl) to the dianionic trinuclear organorhenium complex, as shown by cyclic voltammetry. An irreversible oxidation step occurs at +0.94 V. A single crystal X-ray diffraction study was performed to determine the structure of $[Cp_2Co][Me_6Re_3O_6]$ (**4**) (*vide infra*).

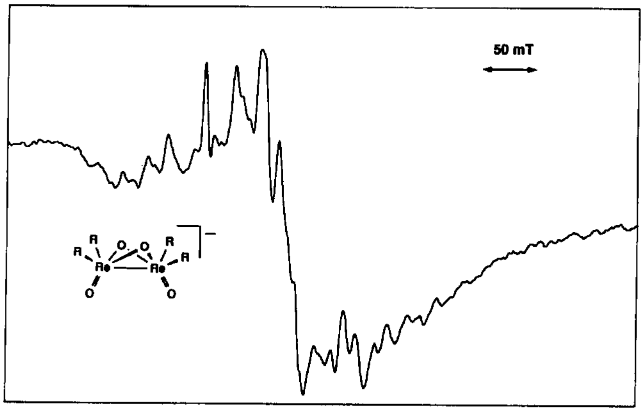

Fig. 3. Anisotropic EPR spectrum (9.0715 GHz) of the radical anion $[Me_4Re_2O_4]^-$ (**1**$^-$) in MeCN at 115 K.

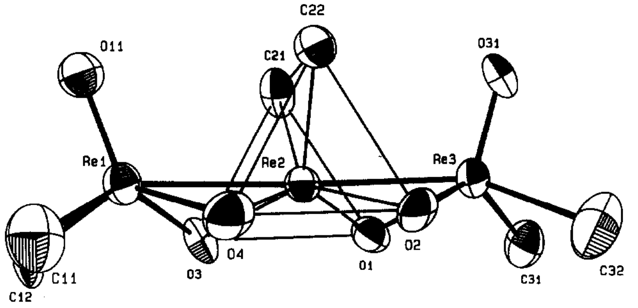

Fig. 4. ORTEP drawing of the trinuclear clusteranion $[Me_6Re_3O_6]^-$.

The proposed mechanism of the formation of the trinuclear complex **4** is illustrated in Scheme 1. The formation of a μ-(O$_2$)-bridged intermediate is proposed, as for the reaction of $(\eta^5\text{-}C_5Me_5)_2Re_2O_4$ with

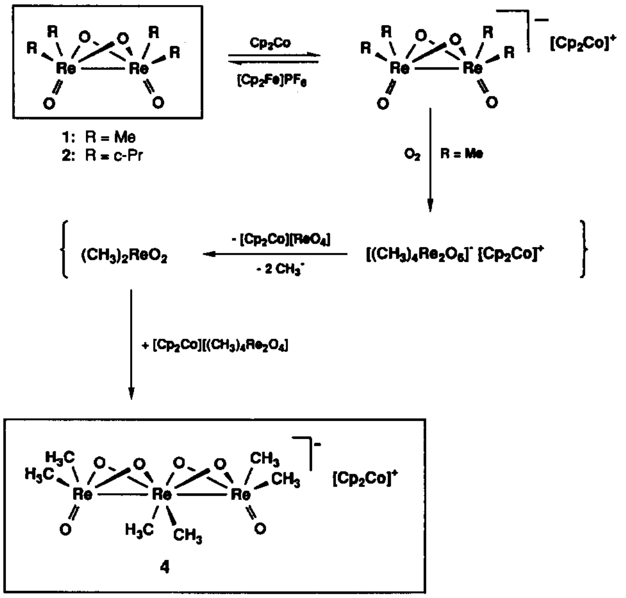

Scheme 1.

TABLE 2. Crystal data and details of data collection and refinement for **4**

Formula	$C_{16}H_{28}O_6Re_3Co$
Molecular weight (a.m.u.)	933.9
Crystal colour and habit	purple, irregular fragment
Temperature (°C)	(23 ± 3)
Space group	monoclinic $P2_1/n$ (Int. Tab. (non-standard) Nr. 14)
a (pm)	933.8(3)
b (pm)	1174.0(1)
c (pm)	2020.3(4)
β (°)	91.38(1)
V (pm^3)	$2214 \cdot 10^6$
Z	4
δ (calcd) (g cm^{-3})	2.801
Radiation	Mo Kα; $\lambda = 71.07$ pm
Max. scan time (s)	90
Max. 2θ (°)	50
Total number of refl.	3772; $h(-11/11)$; $k(0/13)$; $l(0/24)$
Unique refl.	3002
Used refl.	2999 with $I > 0.01\sigma(I)$
Used method	Patterson
Hydrogens	calculated, not refined
Refined parameters	225
R	0.051
R_w	0.035
Goodness of fit	2.525
Residual electron dens. (e/Å^3)	+2.17; 125 pm from Re3, −1.83; 98 pm from Re1.
Absorption corr., μ (cm^{-1})	empirical; 173.4
Transmission	0.1334–0.9998

TABLE 3. Final positional parameters for non-hydrogen atoms and equivalent temperature factors (Å^2) with esd's in parentheses for **4**

Atom	x	y	z	B_{eq}
Re1	0.21932(8)	0.12126(5)	0.92821(3)	2.79(1)
Re2	0.43631(7)	0.20057(4)	0.85999(3)	2.34(1)
Re3	0.65472(8)	0.27209(4)	0.78987(3)	3.00(1)
Co	0.6822(3)	0.3817(2)	0.10803(9)	3.57(5)
O1	0.598(1)	0.2991(7)	0.8802(4)	3.0(2)
O2	0.451(1)	0.2754(7)	0.7754(4)	4.0(3)
O3	0.374(1)	0.2238(7)	0.9505(4)	2.9(2)
O4	0.230(1)	0.2007(7)	0.8447(4)	4.0(3)
O11	0.228(1)	−0.0212(7)	0.9323(4)	3.5(2) [a]
O31	0.757(1)	0.1610(8)	0.7667(5)	5.3(3)
C11	0.003(2)	0.147(1)	0.9089(7)	5.1(5)
C12	0.163(2)	0.165(1)	1.0266(7)	4.5(4)
C21	0.576(2)	0.076(1)	0.9090(7)	3.4(4)
C22	0.423(2)	0.051(1)	0.7980(7)	3.4(4)
C31	0.813(2)	0.391(1)	0.8178(8)	4.1(4)
C32	0.642(2)	0.371(1)	0.7015(8)	6.0(5)
C41	0.563(2)	0.248(1)	0.1337(8)	4.7(4)
C42	0.612(2)	0.303(1)	0.1903(8)	6.4(5)
C43	0.561(2)	0.413(2)	0.1868(8)	6.5(5)
C44	0.488(3)	0.428(1)	0.126(1)	7.0(6)
C45	0.481(2)	0.322(1)	0.0952(7)	5.0(5)
C51	0.847(2)	0.493(2)	0.1079(8)	7.0(6)
C52	0.898(3)	0.381(2)	0.114(1)	7.3(5) [a]
C53	0.852(3)	0.320(2)	0.060(1)	10.9(8)
C54	0.765(2)	0.391(2)	0.0157(8)	6.9(6)
C55	0.765(2)	0.501(2)	0.0492(9)	5.9(5)

[a] Refined isotropically.

dioxygen [21]. The unstable intermediate loses methyl radicals, which combine to give ethane or abstract hydrogen atoms from the solvent to give methane. Other products are cobaltocenium perrhenate and probably the very reactive electrophile $Me_2Re^{VI}O_2$. An analogous electron deficient Re^{VI} compound stabilized by two σ-mesityl groups is known [22]. Insertion

TABLE 4. Selected bond lengths (pm) and angles (°) in **4**

Re1–Re2	2.6470(6)	Re2–O2	1.929(5)
Re1–O3	1.926(7)	Re2–O3	1.951(6)
Re1–O4	1.932(6)	Re2–O4	1.946(7)
Re1–O11	1.676(6)	Re2–C21	2.176(9)
Re1–C11	2.07(1)	Re2–C22	2.162(8)
Re1–C12	2.14(1)	Re3–O1	1.937(6)
Re2–Re3	2.6479(6)	Re3–O2	1.920(8)
Re2–O1	1.940(7)	Re3–O31	1.687(7)
Re2–Re1–O11	109.9(2)	O1–Re2–C21	81.3(4)
Re2–Re1–C11	127.3(3)	O2–Re2–O4	87.1(3)
O3–Re1–O4	81.3(3)	O2–Re2–O3	142.7(2)
O4–Re1–C11	80.5(4)	O3–Re2–O4	80.3(3)
O11–Re1–C11	101.6(4)	C21–Re2–C22	75.2(4)
O11–Re1–C12	101.9(4)	Re2–Re3–O31	110.5(2)
C11–Re1–C12	83.0(4)	O1–Re3–O2	81.4(3)
Re1–Re2–Re3	177.83(3)	O31–Re3–C31	100.9(4)
O1–Re2–O3	88.2(2)	O31–Re3–C32	102.1(4)
O1–Re2–O4	142.9(2)	C31–Re3–C32	83.5(4)

of this intermediate into the dimeric structure of the radical anion 1^- would account for the formation of the linear trinuclear mixed-valence anion. To date, similar reactions with 2^- have not given an analogous trinuclear rhenium cluster; steric factors could be responsible for the inhibition of the reaction in this case.

3.4. *Crystal structure of $[Me_6Re_3O_6]^-$*

A view of the linear trimeric anion is shown in Fig. 4. Selected bond distances and angles are summarized in Table 2. The trimeric anion has almost C_{2v} symmetry. The central rhenium atom is in a distorted trigonal prismatic environment consisting of four bridging oxygen ligands and two terminal methyl groups. The coordination geometry of both the outer rhenium atoms is square pyramidal, as in the dimeric starting material **1** [23]. The Re–Re–Re linkage is nearly linear (177.83(2)°). The rhenium–rhenium distances (264.70(6), 264.79(6)) are 5 pm longer than that in **1**, and correspond to rhenium–rhenium single bonds [24]. The middle rhenium atom (Re(2)) is surrounded by two methyl and four oxo groups in a distorted trigonal prismatic ligand arrangement. The bond angle C–Re–C at the central rhenium atom (75.2°(4)) is narrower than the corresponding angles at the terminal rhenium atoms Re(1) (83.0(4)°) and Re(3) (83.5(4)°) or in structurally related bis-alkyl complexes such as $[Np_2ReO_2]_2$ (**3**) (80.3(10)°, 81.9(11)°)), $\{[Li(NCCH_3)_2][Np_2ReO_2]\}_2$ (83.7(5)°) and $\{[(C_2H_5)_4N][Np_2ReO_2]\}$ (81.2(5)°) [8].

4. Conclusion

The electrochemical reduction of **1** and **2** gives in a quasi-reversible step the mixed-valence dimeric radical anions $[Cp_2Co][Me_4Re_2O_4]$ (1^-) and $[Cp_2Co][c\text{-}Pr_4Re_2O_4]$ (2^-). Oxidation of 1^- can follow either of two pathways depending on the nature of the oxidizing reactant: "outer sphere" oxidizing agents such as ferricinium salts regenerate the starting compound **1**, whereas dioxygen gives, via an oxidative aggregation process, the trinuclear cluster $[Cp_2Co][Me_6Re_3O_6]$ (**4**). Formation of this cluster seems to depend on steric effects, since no oxidative aggregation is observed for $[2]^-$. Interestingly, formation of a linear cluster is favoured over aggregation to a cyclic trimeric cluster such as $[(\eta^5\text{-}C_5Me_5)_3Re_3O_6]^{2+}$ [21].

Acknowledgments

The authors thank Prof. W.A. Herrmann (TU München) for his support and discussion, and Dr. H.T. Huy for providing compound **2**. Financial support for this work by the Studienstiftung (fellowship to R.W.A.), The Hans-Seidel-Stiftung (fellowship to J.B.), the German-French Procope program, the Deutsche Forschungsgemeinschaft, and the Degussa AG (loan on Re_2O_7) are gratefully acknowledged.

References and notes

1 R. H. Holm, *Chem. Rev., 87* (1987) 1401.
2 (a) W. A. Herrmann, *Kontakte (Darmstadt), 1* (1991) 22; (b) W. A. Herrmann, *Kontakte (Darmstadt), 3* (1991) 29.
3 W. A. Herrmann, P. Kiprof, K. Rypdal, J. Tremmel, R. Blom, R. Alberto, J. Behm, R. W. Albach, H. Bock, B. Solouki, J. Mink, D. Lichtenberger and N. E. Gruhn, *J. Am. Chem. Soc., 113* (1991) 6527.
4 R. W. Albach, *Ph.D. thesis*, TU München, Garching, 1992.
5 U. Küsthardt, *Ph.D. thesis*, TU München, Garching, 1986.
6 W. A. Herrmann, R. W. Albach and J. Behm, *J. Chem. Soc., Chem. Commun.*, (1991) 367.
7 H. T. Huy in F. Kühn, *Diploma thesis*, TU München, Garching, 1992.
8 S. Cai, D. M. Hoffman, J. C. Huffman, D. A. Wierda and H.-G. Woo, *Inorg. Chem., 26* (1987) 3693.
9 K. Jung, *Ph.D. thesis*, TU München, Garching, 1990.
10 M. D. Rausch and H. B. Gordon, *J. Organomet. Chem., 74* (1974) 85.
11 W. M. Amslinger, *Ph.D. thesis*, TU München, Garching, 1991.
12 (a) D. T. Cromer and J. T. Waber, *International tables of Crystallography*, Vol. IV, Tab. 2.2.B, Kynoch Press, Birmingham/England, 1978; (b) D. T. Cromer and J. B. Mann, *Acta Crystallogr. (Copenhagen), Sect. A, 24* (1968) 321.
13 (a) D. T. Cromer, *International tables of Crystallography*, Vol. IV, Table 2.3.1, Kynoch Press, Birmingham/England, 1974; (b) D. T. Cromer and D. Liberman, *J. Chem. Phys., 53* (1970) 1891.
14 Me_4ReO, $Me_6Re_2O_3$, Mes_2ReO_2, $Me_4Re_2O_4$ and $c\text{-}Pr_4Re_2O_4$ are described in Ref. 4.
15 R. S. Nicholson and I. Shain, *Anal. Chem., 36* (1964) 706.
16 For **1**: $\Psi = -0.18 + 0.50\ \upsilon^{-1/2}$ ($\upsilon = 0.06\text{–}0.8\ V\ s^{-1}$); $D = 3.45 \cdot 10^{-5}\ cm^2\ s^{-1}$.
17 $\Psi = k_s{}^0(D\upsilon\pi nE_{th}{}^{-1})^{-1/2}$, $E_{th} = RTF^{-1} = 25.5$ mV.
18 J. L. Sadtler and A. J. Bard, *J. Am. Chem. Soc., 90* (1968) 1979.
19 Extrapolated to infinite dilution.
20 W. J. Geary, *Coord. Chem. Rev., 7* (1971) 81.
21 W. A. Herrmann, R. Serrano, U. Küsthardt, E. Guggolz, B. Nuber and M. L. Ziegler, *J. Organomet. Chem., 287* (1985) 329.
22 P. Stavropoulos, P. G. Edwards, T. Behling, G. Wilkinson, M. Motewalli and M. B. Hursthouse, *J. Chem. Soc., Dalton Trans.*, (1987) 169.
23 W. A. Herrmann, J. G. Kuchler, W. Wagner, J. K. Felixberger and E. Herdtweck, *Angew. Chem., Int. Ed. Engl., 27* (1988) 294.
24 W. A. Herrmann, *J. Organomet. Chem., 300* (1986) 111.
25 $[(\eta^5\text{-}C_5Me_5)_3Re_3O_6](BF_4)_2$: U. Küsthardt and W. A. Herrmann, unpublished results; $[(\eta^5\text{-}C_5Me_5)_3Re_3O_6](ReO_4)_2$: see Ref. 21.